

Methodology for Avoidance of Ratcheting-Induced Stable Cracking (RISC) in Microelectronic Devices

Zhen Zhang, Zhigang Suo

Division of Engineering and Applied Sciences, Harvard University, Cambridge, MA 02138

Yong Liu, Scott Irving, Timwah Luk and Don Desbiens

Fairchild Semiconductor Corp., 82 Running Hill Road, Mail Stop 35-2E, ME 04106

Email: yliu@fairchildsemi.com; Tel: (207) 761-3155; Fax: (207) 761-6339

Abstract

A typical microelectronic device contains a silicon die in a package encapsulated with an epoxy. This polymer and various inorganic materials on the die, such as metal interconnects and ceramic passivation films, have dissimilar coefficients of thermal expansion (CTEs). When such a device is subject to a change in temperature, the mismatch in the CTEs deforms the materials. In particular, as temperature cycles, the plastic deformation in a metal interconnect may accumulate incrementally, a phenomenon known as *ratcheting plastic deformation*. Ratcheting in the metal film may induce large stresses in an overlying ceramic film, causing cracks to initiate and grow stably cycle by cycle. In this paper, such *ratcheting-induced stable cracking* (RISC) is studied using a simplified three-layer model. We describe conditions under which ratcheting will occur in the metal layer, predict the number of cycles for the crack to initiate in the ceramic film, and discuss strategies to avoid RISC in design.

Introduction

D-PAK is an electronic package widely used in automobile and power industry. Its structure is representative of many electronic packages that integrate diverse materials, as illustrated in Fig. 1. On a silicon wafer, layers of polysilicon gates and dielectrics are deposited, which in turn are covered by metal interconnect, and then passivated by a SiN film. The wafer is then cut into dies, each of which is then mounted on a copper pad and encapsulated with an epoxy molding compound (EMC) at 175°C.

Due to mismatch between the coefficients of thermal expansion (CTEs), such an electronic package may exhibit various modes of failure in a thermal-cycling test. As an example, Fig. 2 shows the micrographs of a D-PAK after 1000 cycles between -65°C and 150°C. Cracks occur near the edges in the SiN film over wide aluminum pads, but rarely in the SiN film over narrow aluminum rings. These cracks typically initiate after some number of cycles, and grow stably cycle by cycle [1-4]. This failure mode is known as ratcheting-induced stable cracking (RISC).

This paper studies RISC using a simplified three-layer model. We will elaborate the failure mechanism, describe conditions under which ratcheting will occur in the metal layer, predict the number of cycles for the crack to initiate in the ceramic film, and discuss strategies to avoid RISC in design.

Ratcheting-Induced Stable Cracking: a Synopsis

This section describes qualitatively the process of RISC, leaving quantitative aspects to later sections. Fig. 3 illustrates

the structure to be studied as a model of the D-PAK. The passivation film, thickness h , lies on the metal underlayer, thickness H , which in turn lies on the semi-infinite substrate. The passivation film is elastic, the underlayer is elastic-perfectly-plastic, and the substrate is also elastic. Both a blanket metal film and a metal stripe are considered here. The gates and BPSG are just thin layer above silicon, and do not significantly affect the deformation of aluminum and passivation films. Consequently, the gates and BPSG are treated as a part of the substrate.

The EMC has a larger CTE than the silicon die. Upon cooling from the curing temperature, if the EMC board and the silicon die were separated, the EMC would contract more than the silicon. However, this relative motion is constrained by the bonding between the EMC and the die, so that shear stresses develop on the EMC/die interface, concentrating at

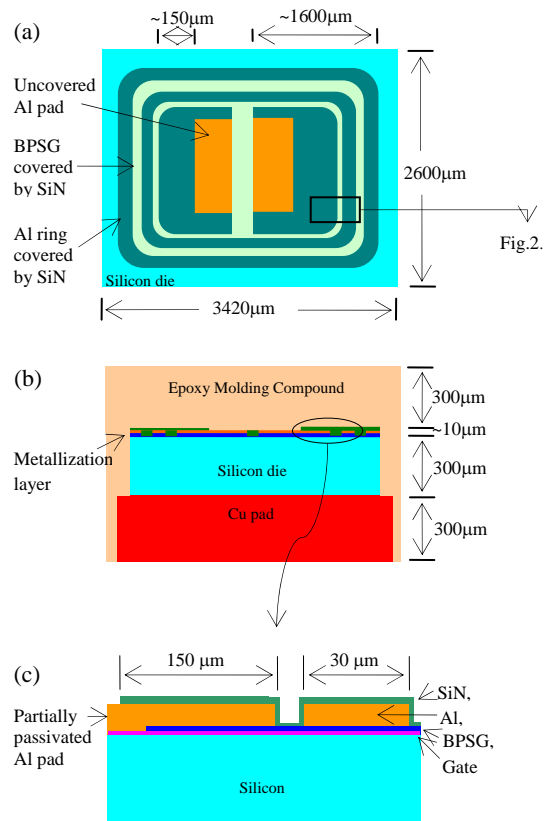


Fig. 1. Schematics of a D-PAK structure. (a) Top view. (b) Cross section. (c) Magnified view of the interconnect structure of the lower right corner.

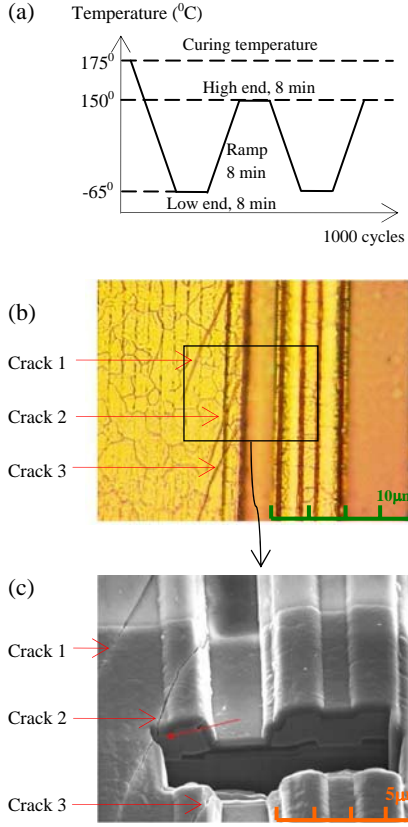


Fig. 2. (a) Temperature history in a thermal-cycling test. (b) Optical micrograph of a fractured die surface after 1000 temperature cycles. (c) SEM micrograph with a FIB cut.

the edges and corners of the die. During a thermal-cycling test, the high-end temperature (150°C) is lower than the curing temperature (175°C). Consequently, at each corner or edge of the die, the magnitude of the shear stress varies with the temperature, but the direction of the shear stress is always biased towards the center of the die. We denote the shear stress on the EMC/die interface by τ_0 , as indicated in Fig. 3.

This interfacial shear stress τ_0 is partly sustained by the passivation film as a membrane stress σ , and partly transmitted to the metal film as a shear stress τ_m [1-3]. The shear stress τ_m in the metal, being limited by the yield strength of the EMC, may or may not be high enough to cause the metal film to undergo plastic deformation. However, the metal film also has a larger CTE than silicon, so that the normal stress in the plane of the metal film, σ_m , changes with temperature. If this in-plane stress causes the metal to yield in every cycle, τ_m will cause plastic shear strain in the same direction as τ_m (i.e., toward the center of the die), no matter how small τ_m is. Under this condition, the plastic shear strain in the metal will accumulate cycle by cycle, a phenomenon known as ratcheting plastic deformation [5].

As it ratchets toward the center, the metal film carries the overlying passivation film along. However, if the passivation film is bonded with the die along an edge, the

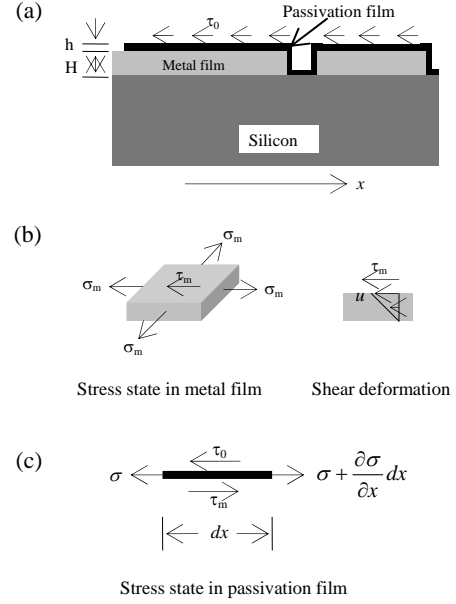


Fig. 3. (a) A partially passivated blanket film. (b) The stress state in the metal film and shear deformation. (c) The stress state in the passivation film.

edge will be anchored and move negligibly. Consequently, the ratcheting metal will elastically deform the passivation and build up the membrane stress in the passivation.

The magnitude of the membrane stress in the passivation can be very high. This is understood as follows. The interfacial shear stress τ_0 is due to the mismatch in the CTEs of the epoxy and the silicon, so that the magnitude of τ_0 will not decay with the cycles. Recall that the interfacial shear stress τ_0 is partly sustained by the passivation film as the membrane stress σ , and partly transmitted to the metal film as the shear stress τ_m . As the metal film ratchets, the membrane stress in the passivation builds up, but the magnitude of the shear stress in the metal τ_m decays. After many cycles, τ_m will vanish, and τ_0 is fully sustained by the membrane stress in the passivation. The structure is said to have reached the *steady state*.

Fig. 4 plots the steady-state distribution of the membrane stress in the passivation film for two kinds of geometry. In Fig. 4(a), both ends of the passivation film are anchored to the silicon die, so that the membrane stress is tensile on the right side, and compressive on the left. At the two edges of the film, the magnitude of the membrane stress is largest, given by

$$\sigma_{ss} = \frac{\tau_0 L}{h}, \text{ at } x = L \quad (1)$$

This equation is obtained by the balance of the forces acting on the passivation film. In Fig. 4(b), the right end is anchored, but the left end is free, so that the membrane stress vanishes on the left end, and linearly builds up toward the right. The magnitude of the stress at the right end is still given by (1).

Equation (1) shows that, even if the magnitude of the interfacial shear stress τ_0 is modest, the large aspect ratio

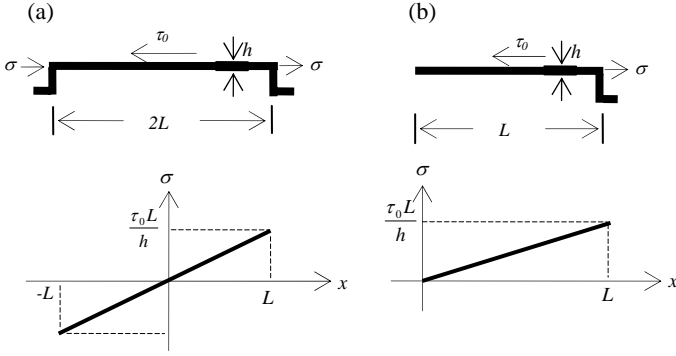


Fig. 4. Stress distribution in steady state for both fully passivated and partially passivated SiN films. (a) Two ends are fixed. (b) One end is fixed, the other free.

L/h can greatly amplify the magnitude of the membrane stress. This is known as the shear-lag effect. When the tensile stress in the passivation is high enough, cracks will initiate and grow stably cycle by cycle. The following sections consider various aspects discussed above more quantitatively.

Ratcheting in Metal Films

To better understand ratcheting plastic deformation, we next consider a blanket metal film on a silicon substrate, subject to cyclic temperature between T_L and T_H . For the time being, we assume that the shear stress τ_m is uniform in the metal and invariant with the temperature. The metal film is taken to be elastic-perfectly-plastic, with the CTE α_m , Young's modulus E_m , Poisson's ratio ν_m , and the temperature-independent yield strength Y_m . The substrate is elastic with CTE α_s . As shown in Fig. 3(b), the metal film is under biaxial in-plane stress σ_m due to the temperature change, and a shear stress τ_m . The metal film is elastic when the stresses satisfy the von Mises yield condition:

$$\sigma_m^2 + 3\tau_m^2 < Y_m^2 \quad (2)$$

As the temperature cycles between T_L and T_H , the normal stress σ_m also cycles (Fig. 5). When the metal is plastic, the normal stress is fixed at constant levels $\sigma_m = \pm\sqrt{Y_m^2 - 3\tau_m^2}$. When the metal is elastic, however, the normal stress changes linearly with the temperature, having a slope $E_m(\alpha_m - \alpha_s)/(1 - \nu_m)$. It is evident from Fig. 5, to ensure that the metal film remains elastic after the first cycle, the following condition must be satisfied [2]:

$$\left[\frac{E_m(\alpha_m - \alpha_s)(T_H - T_L)}{2(1 - \nu_m)Y_m} \right]^2 + 3\left(\frac{\tau_m}{Y_m}\right)^2 < 1. \quad (3)$$

Condition (3) is known as the *shakedown* condition. Under this condition the metal film may undergo plastic deformation in part of the first cycle, but will remain elastic in subsequent cycles.

Fig. 6 shows a plane spanned by the normalized shear stress, τ_m/Y_m , and the normalized temperature range, $E_m(\alpha_m - \alpha_s)(T_H - T_L)/(1 - \nu_m)Y_m$. The plane is divided into four

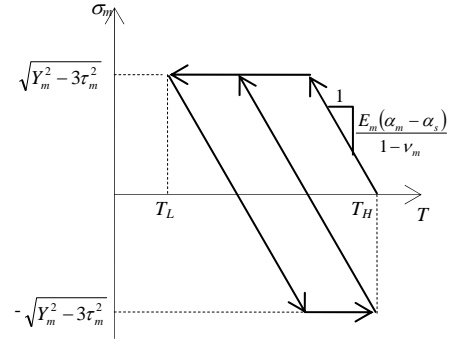


Fig. 5. Biaxial stress in metal film as a function of the temperature.

regimes: shakedown, plastic collapse, cyclic plastic deformation, and ratcheting. Such a diagram is called a Bree diagram [5]. Condition (3) corresponds to part of an ellipse, inside which lies the shakedown regime. As a separate consideration, when $\tau_m/Y_m \geq 1/\sqrt{3}$, the metal film will deform plastically under the shear stress alone without the aid of the temperature change. In the other limit, when $\tau_m = 0$, the metal film undergoes cyclic plastic deformation if the temperature range is sufficiently large. The regime bounded within the above three boundaries is the ratcheting regime, where the metal film yields every cycle, but the amount of plastic shear strain is finite, accumulating cycle by cycle.

We next compare Al and Cu interconnects. As indicated by Table I, the yield strength of EMC is comparable to that of Al, or even larger. Note that the interfacial shear stress τ_0 is linearly proportional to the temperature change when the EMC is elastic, and is limited by the shear yield strength of the EMC when the EMC is plastic. Hence, in this design of D-PAK, if the temperature range is large, τ_0 by itself can cause the Al film to deform plastically.

To avoid plastic collapse, the design has to be modified to decrease the yield strength of the molding compound. Also notice that Al has a large CTE, such that the value of

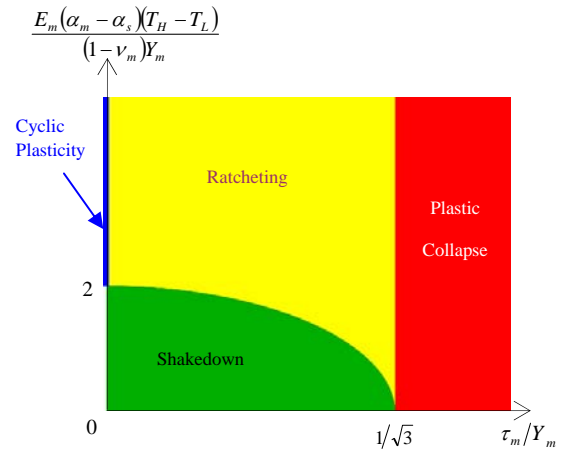


Fig. 6. The Bree diagram for the elastic and perfectly plastic metal film. The plane is divided into four regimes: plastic collapse, shakedown, ratcheting, and cyclic plastic deformation.

TABLE I. Materials properties.

Materials	Young's modulus E (GPa)	Poisson's ratio ν	CTE α (10^{-6} K^{-1})	Yield Strength Y (MPa)	Toughness K_{Ic} ($\text{MPa}\cdot\text{m}^{1/2}$)
EMC	17	0.3	24	98~150	
BPSG	64	0.17	2.78		
Silicon die	162.5	0.22	2.8		
Poly gate	162.5	0.22	2.8		
SiN	275	0.24	4		5.8~8.5
Al	70.34	0.346	23.2	110	
Cu	130	0.33	17	345~310	

$E_m(\alpha_m - \alpha_s)(T_H - T_L)/(1 - \nu_m)Y_m = 4.29 > 2$. Consequently, interfacial shear stress τ_0 of any magnitude can cause ratcheting. Indeed, ratcheting is commonly reported for aluminum interconnects (see Refs cited in [1-3]).

By contrast, ratcheting has not been reported in Cu interconnects. Using the values in Table I, we find for Cu $E_m(\alpha_m - \alpha_s)(T_H - T_L)/Y_m(1 - \nu_m) = 1.77$. Using the yield strength of EMC as an estimate for τ_0 , we find that $\tau_0/Y_m = 0.29$. These two estimates correspond to a point just above the ellipse in Fig. 6, so that the Cu film will ratchet for the beginning cycles. However, the shear stress in Cu, τ_m , will relax from its initial value τ_0 cycle by cycle, so that the Cu film will approach the shakedown regime after a certain number of cycles. If the passivation film does not crack before the Cu film shakes down, it will never crack in the future cycles.

We next consider the plastic strain per cycle. When $E_m(\alpha_m - \alpha_s)(T_H - T_L)/(1 - \nu_m)Y_m > 2$, and the shear stress τ_m is much smaller than its yield strength Y_m , the plastic shear strain rate per cycle versus the shear stress can be approximated by a linear relation [3]:

$$\frac{\partial \gamma^p}{\partial N} = \frac{\tau_m}{\eta}. \quad (4)$$

where N be the number of cycles, and η , the linear ratcheting coefficient, is given as follows:

$$\eta = \frac{E_m}{12(1 - \nu_m)} \left[\frac{E_m(\alpha_m - \alpha_s)(T_H - T_L)}{(1 - \nu_m)Y_m} - 2 \right]^{-1}. \quad (5)$$

For example, if $\tau_m/Y_m < 0.2$, then the error of the linear approximation is less than 10%.

In the temperature range specified in Fig.2(a), all the materials in the structure do not creep, so dwelling time at high end and low end do not affect the analysis. In practice, it takes some time for the structure to reach a state of uniform temperature during the testing, but in the follow analysis, we neglect the nonuniformity in temperature. Consequently, various types of loading program, linear or sinusoidal, dwelling or not, will lead to the same accumulative effects over many cycles.

Cracking in Passivation Films

Let $\sigma(x, N)$ the membrane stress, and $u(x, N)$ the displacement. For simplicity, the interfacial shear stress τ_0 is assumed to be a constant, but the shear stress in the metal is taken to be a function $\tau_m(x, N)$. As shown in Fig. 3(c), the equilibrium of an infinitesimal element of the passivation film requires that $\partial \sigma / \partial x + (\tau_m - \tau_0)/h = 0$. Hooke's law relates the membrane stress to the membrane strain, $\sigma = \bar{E}_p \partial u / \partial x$, where $\bar{E}_p = E_p / (1 - \nu_p^2)$, and E_p and ν_p are Young's modulus and Poisson's ratio of passivation film. Moreover, as shown in Fig. 3(b), the plastic shear strain relates to the displacement as $\gamma^p = u/H$. These relations, combining with Equation (4), give the governing equation for $u(x, N)$:

$$\frac{\partial u}{\partial N} = D \frac{\partial^2 u}{\partial x^2} - \frac{\tau_0 H}{\eta} \quad (6)$$

where $D = hH\bar{E}_p/\eta$. Equation (6) has the same form as the diffusion equation, and D can be interpreted as an effective diffusivity.

The characteristic number of cycles to reach the steady state can be estimated by

$$N_0 = \frac{L^2}{D} = \frac{L^2}{hH} \frac{\eta}{\bar{E}_p} \quad (7)$$

The complete solution of Equation (6) can be written as a series with the initial condition of $u = 0$ at $N = 0$. Because the first term in the series dominates when $N > 0.05N_0$, the maximum tensile stress build-up on the right edge can be approximated by the following:

$$\sigma \approx \frac{\tau_0 L}{h} \left[1 - \frac{8}{\pi^2} \exp\left(-\frac{\pi^2 N}{4 N_0}\right) \right] \quad (8)$$

Note that in this paper we have neglected the residual stress in SiN due to the deposition processes.

Now let us consider an initial crack, of length $2a$, in the blanket passivation film, as shown in Fig. 7. As the aluminum layer ratchets, the membrane stress in the passivation film builds up globally over the length scale L . However, locally near the crack, over the length scale a , the membrane stress relaxes. We can identify two distinct *cycle scales*. The

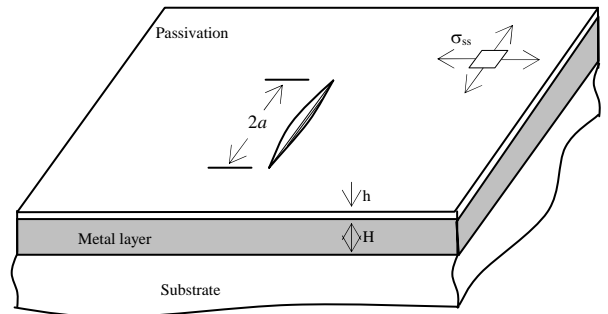


Fig. 7. A schematic of a finite initial crack, of length $2a$, in the passivation film.

number of cycles to attain the steady state over the width of the passivation L scales as L^2/D . The number of cycles to relax near the crack scales as a^2/D . Assuming, $L \gg a$, after many cycles, the crack behaves like a Griffith crack [6-11]. When the membrane stress is σ , the stress intensity factor is given by

$$K = \sigma\sqrt{\pi a}. \quad (9)$$

If this stress intensity factor is below the fracture toughness K_c of the passivation, i.e., $\sigma\sqrt{\pi a} < K_c$, the crack does not grow. Consequently, the fracture strength of the passivation σ_c is given by $\sigma_c = K_c/\sqrt{\pi a}$. In particular, if the fracture strength exceeds the steady state stress at the edge of the passivation, given by Equation (1), the crack will never grow. This condition is given by

$$\sigma_c > \tau_0 L/h. \quad (10)$$

When Condition (10) is violated, however, the crack will initiate to grow after a certain number of cycles, denoted by N_i . Using Equation (8), we obtain that

$$\frac{N_i}{N_0} = -\frac{4}{\pi^2} \ln \left[\frac{\pi^2}{8} \left(1 - \frac{\sigma_c h}{\tau_0 L} \right) \right]. \quad (11)$$

This equation is valid when N_i is sufficiently large. Fig. 8 plots the normalized number of cycles to crack initiation versus the normalized stress level in steady state. The whole plane is divided into two regimes: no crack initiation and delayed cracking as Equation (11).

Using the values in Table I and Fig. 1, and the shear stress $\tau_0 = 50$ MPa, the stress at steady state is $\sigma_{ss} = 5$ GPa at the edge of the middle blanket film, and the characteristic number of cycles is about $N_0 = 50$. From Table I, if we use $5.8 \text{ MPa}\cdot\text{m}^{1/2}$ as the fracture toughness of SiN, and assume the largest initial crack length is comparable to the thickness, $1.5 \mu\text{m}$, then the critical stress to initiate the crack would be

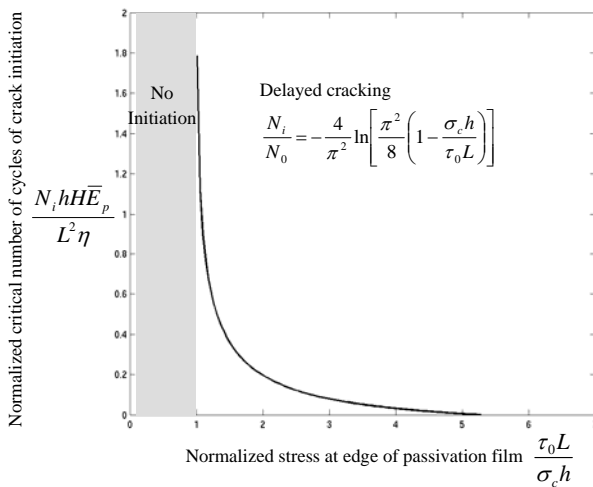


Fig. 8. Normalized critical number of cycles to initiate the crack versus the normalized steady state stress level. If the steady state stress level is less than fracture strength, the crack remains stationary; otherwise, the crack initiates and grows after delayed cycles.

$\sigma_c = 4.73$ GPa. Hence, from Fig. 8 and Eq.(11), it takes at least 55 cycles for crack initiation. In the narrow stripe, $\sigma_{ss} = 500$ MPa at the edge, so that cracking is less likely to happen. The above conclusion can be verified by experimental pictures in Fig. 2.

In the case of Fig.4(a), if the crack size is comparable or larger than the width of the stripe, then the stress intensity factor is determined by $K \sim \sigma_{ss}\sqrt{L}$, and so there exists a critical width of the stripe [9]:

$$L_c \sim \left(\frac{K_c h}{\tau_0} \right)^{2/3}. \quad (12)$$

below which the crack never grow no matter how long the crack is. Based on this equation, and put the value in, we can estimate that the critical width is $50 \mu\text{m}$ for fully passivated stripe.

Design Modifications

From the above study, we may consider the following design modifications to avoid passivation cracking.

A. Buffer layer

If we add a compliant and soft buffer layer between EMC and silicon die, the shear stress τ_0 can reduce significantly, and so does the stress level in steady state. Correspondingly, the lower bound of critical number of cycles of crack initiation, N_i , can increase by several orders of magnitude. It is even possible to prevent crack initiation. The comparisons are plotted in Fig. 9 and Fig. 10.

B. Small passivation width

The reduction of width and length and the increase of thickness of passivation also can reduce the stress level. The change of large or long passivation film to small or narrow pads is a practical method, for example, introducing slots into the passivation film. In Fig.11, a lower right corner is simulated by ANSYS. The original design, the design with slots, and the narrow stripe are shown. The stress level at steady-state is significantly reduced in the latter two cases.

Conclusion

Ratcheting-induced stable cracking (RISC) in passivation film is a commonly observed failure mode in microelectronic devices. This paper uses a 1-D model to estimate the lifetime in terms of temperature cycles, and to establish conditions that avoid this failure mode. A Bree-type diagram is plotted to ascertain if a metal film will undergo ratcheting plastic deformation. Under the condition that the metal does ratchet, we estimate the number of cycles for cracks to initiate. Several possible design modifications are discussed.

Acknowledgement

This work is done under the co-op project of Fairchild Semiconductor Corporation.

Reference

1. M. Huang, Z. Suo, Q. Ma, and H. Fujimoto, "Thin film cracking and ratcheting caused by temperature cycling," *J. Mater. Res.*, vol. 15, no. 6, pp. 1239-1242, 2000.

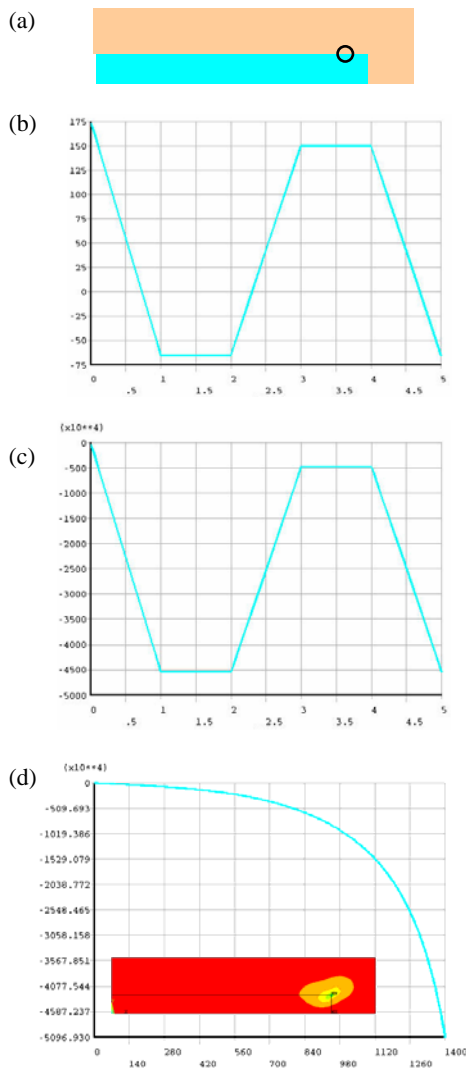


Fig. 9. (a) The schematic of upper right quarter of the die package. (b) The temperature loading profile with unit $^{\circ}\text{C}$. (c) The interfacial shear stress evolution around the corner as shown in (a) by circle, unit Pa. (d) Interfacial shear stress along the interface at $T=-65^{\circ}\text{C}$ with unit Pa, and the inset shows the contour plot of FEA calculation.

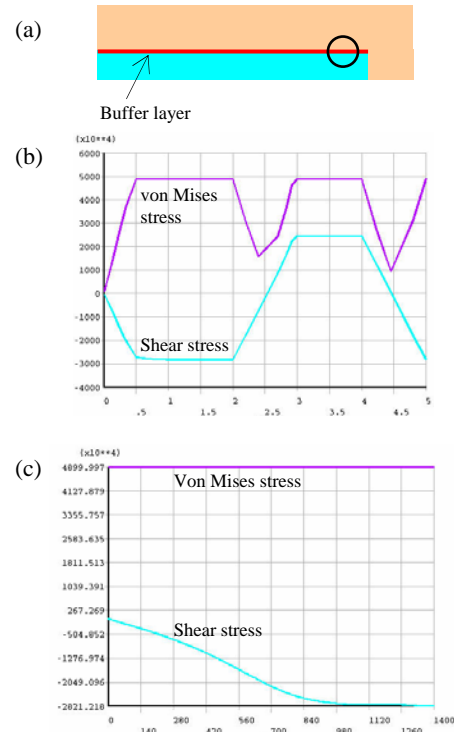


Fig. 10. (a) The schematic of upper right quarter of the die package with buffer layer, under the same loading condition as in Fig.9(b). (b) The evolution of interfacial shear stress and von Mises stress around the corner as shown in (a) by circle, unit Pa. (c) Interfacial shear stress and von Mises stress along the interface at $T=-65^{\circ}\text{C}$ with unit Pa.

- M. Huang, Z. Suo, and Q. Ma, "Metal film crawling in interconnect structures caused by cyclic temperatures," *Acta Mater.*, vol. 49, pp. 3039-3049, 2001.
- M. Huang, Z. Suo, and Q. Ma, "Plastic ratcheting induced cracks in thin film structures," *J. Mech. Phys. Solids*, vol. 50, pp. 1079-1098, 2002.
- Z. Zhang, J.H. Prévost, and Z. Suo, "Cracking in interconnects induced by thermal ratcheting," MRS fall meeting, Boston, MA, Dec. 2004.
- J. Bree, "Elastic-plastic behavior of thin tubes subjected to internal pressure and intermittent high-heat fluxes with application to fast-nuclear-reactor fuel elements. *J. Strain Analysis* 2, 226-238.
- Z.C. Xia, and J.W. Hutchinson, "Crack patterns in thin films," *J. Mech. Phys. Solids*, vol. 48, pp. 1107-1131, 2000.

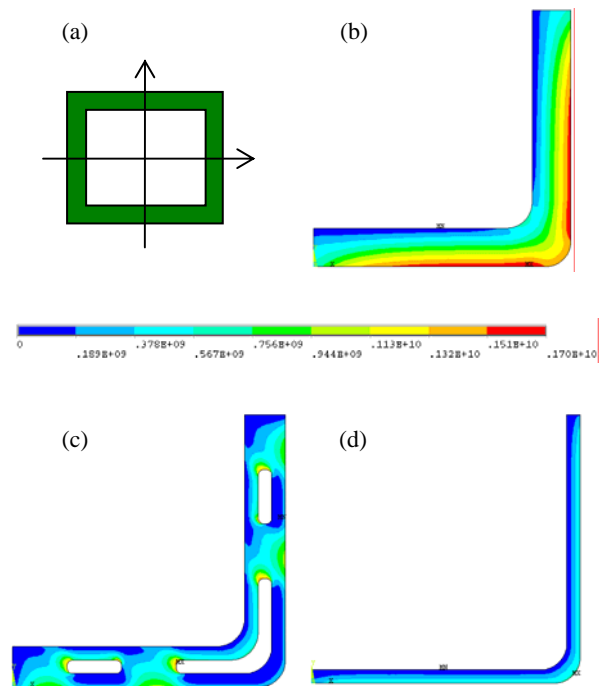


Fig. 11. First principal stress distribution of the passivation film in steady state. (a) Schematic of passivation, due to symmetry only a quarter is calculated. (b) The original design with width $150\mu\text{m}$. (c) The design with some slots. (d) The reduction in width to $50\mu\text{m}$.

7. R. Huang, J.H. Prévost, and Z. Suo, "Loss on constraint on fracture in thin film structures due to creep," *Acta Materialia*, vol. 50, pp. 4137-1448, 2002.
8. J. Liang, R. Huang, J.H. Prévost, and Z. Suo, "Evolving crack patterns in thin films with the extended finite element method," *Int. J. Solids Structures*, vol. 40, pp. 2343-2354, 2003.
9. J. Liang, R. Huang, J.H. Prévost, and Z. Suo, "Thin film cracking modulated by underlayer creep," *Experimental Mechanics*, vol. 43, pp. 269-279, 2003.
10. J. Liang, Z. Zhang, J.H. Prévost, and Z. Suo, 2004, "Time-dependent crack behavior in an integrated structure." *Int. J. Fracture*, vol. 125, pp. 335-348, 2004.
11. Z. Suo, J.H. Prévost, and J. Liang, "Kinetics of crack initiation and growth in organic-containing integrated structures," *J. Mech. Phys. Solids*, vol. 51, pp. 2169-2190, 2003.

